

# A novel POSS-coated quantum dot for biological application

Sarwat B Rizvi<sup>1</sup>  
Lara Yildirimler<sup>1</sup>  
Shirin Ghaderi<sup>1</sup>  
Bala Ramesh<sup>1</sup>  
Alexander M Seifalian<sup>1,2</sup>  
Mo Keshtgar<sup>1,2</sup>

<sup>1</sup>UCL Centre for Nanotechnology and Regenerative Medicine, Division of Surgery and Interventional Science, University College London, United Kingdom; <sup>2</sup>Royal Free Hampstead NHS Trust Hospital, London, United Kingdom

→ Video abstract



Point your SmartPhone at the code above. If you have a QR code reader the video abstract will appear. Or use:  
<http://dx.doi.org/10.2147/IJN.S28577>

Correspondence: Alexander M Seifalian  
University College London,  
United Kingdom  
Tel +44 20 7830 2901  
Email [a.seifalian@ucl.ac.uk](mailto:a.seifalian@ucl.ac.uk)

**Abstract:** Quantum dots (QDs) are fluorescent semiconductor nanocrystals that have the potential for major advancements in the field of nanomedicine through their unique photophysical properties. They can potentially be used as fluorescent probes for various biomedical imaging applications, including cancer localization, detection of micrometastasis, image guided surgery, and targeted drug delivery. Their main limitation is toxicity, which requires a biologically compatible surface coating to shield the toxic core from the surrounding environment. However, this leads to an increase in QD size that may lead to problems of excretion and systemic sequestration. We describe a one pot synthesis, characterization, and in vitro cytotoxicity of a novel polyhedral oligomeric silsesquioxane (POSS)-coated CdTe-cored QD using mercaptosuccinic acid (MSA) and D-cysteine as stabilizing agents. Characterization was performed using transmission electron microscopy Fourier transform infrared spectroscopy, and photoluminescence studies. POSS-coated QDs demonstrated high colloidal stability and enhanced photostability on high degrees of ultraviolet (UV) excitation compared to QDs coated with MSA and D-cysteine alone ( $P$  value  $< 0.05$ ). In vitro toxicity studies showed that both POSS and MSA-QDs were significantly less toxic than ionized salts of Cd<sup>+2</sup> and Te<sup>-2</sup>. Confocal microscopy confirmed high brightness of POSS-QDs in cells at both 1 and 24 hours, indicating that these QDs are rapidly taken up by cells and remain photostable in a biological environment. We therefore conclude that a POSS coating confers biological compatibility, photostability, and colloidal stability while retaining the small size and unique photophysical properties of the QDs. The amphiphilic nature of the coating allows solubility in aqueous solutions and rapid transfer across cell membranes, enabling the use of lower concentrations of the QDs for an overall reduced toxicity particularly for prolonged live cell and in vivo imaging applications.

**Keywords:** quantum dots, polyhedral oligomeric silsesquioxane, surface coating, cytotoxicity

## Introduction

Nanomaterials have dimensional analogies similar to physiological molecules such as proteins and nucleic acids<sup>1</sup> and therefore have been exploited in various biomedical applications, such as tissue engineering, biosensing, medical diagnostics, and therapeutics. At nanoscale sizes, the properties of bulk matter change considerably, giving nanomaterials superior mechanical, thermal, electrical, magnetic, and optical properties that can be exploited extensively in the field of biomedicine. Of the many nanomaterials, particles  $< 100$  nm in diameter are defined as nanoparticles and are of considerable interest to the biomedical scientist. Nanoparticles may be conjugated to biological molecules and incorporated into drug carrier systems, mechanical scaffolds for tissue engineering, and use as contrast agents for in vivo real time imaging applications.<sup>2-6</sup>

Quantum dots (QDs) are fluorescent nanoparticles of semiconductor material with unique photophysical properties that give them significant advantages over organic dyes and proteins commonly used in biomedical imaging.<sup>7</sup> QDs can be size tuned to emit at variable wavelengths ranging all the way from the ultraviolet UV to the near infrared (NIR). Having a broad absorption and narrow emission spectrum, they can be used for multiplexed imaging as differently colored QDs can be excited by the same wavelength of light<sup>1,8,9</sup> provided this wavelength is less than their absorption onset. The QD surface carries free reactive groups that allow biofunctionalization for their targeted delivery. These properties, along with their higher sensitivity, quantum yields, photostability, chemical stability, molar extinction coefficients, and slow decay rates make them ideal probes for real time, long term, and multimodal biomedical imaging.

The most commonly synthesized QDs are based on cadmium salts (eg, cadmium telluride and cadmium selenide), which are coated by a material of a higher band gap, eg, zinc sulphide or cadmium sulphide.<sup>10,11</sup> Furthermore, most QDs are organically synthesized and are insoluble in aqueous media, which makes them inapplicable to biological scenarios. Although QDs can now be aqueously synthesized, their toxicity limits their biomedical application. QD toxicity is multifactorial and is determined by their physiochemical properties, including composition of the core, size, surface charge, concentration, surface chemistry, bioactivity, oxidative, photolytic and mechanical stability, as well as their environmental interactions.<sup>12</sup> The main mechanism of toxicity is the release of free divalent cadmium ions into the surrounding environment through the effects of core oxidation due to the surface coating, which is inadequate or unstable to shield the core from the surrounding oxidative environment. However, the surface coating increases QD size and leads to sequestration in organs of the reticuloendothelial system, including the liver and spleen as they are too large for renal excretion.<sup>13</sup> The liver is the main target of cadmium toxicity, and since larger QDs accumulate in the liver, this effect is likely to be accentuated.

Over the last decade, QD toxicity and surface coatings to render them biologically compatible have been intensively researched. Various materials have been used to protect the QD core from the effects of an oxidative biological environment,<sup>9,14,15</sup> but there are problems of toxicity of the surface coating itself, which is prone to instability and biodegradation. Moreover, surface coating may lead to an overall increase in QD size, which relies on the method of coating, including ligand exchange or ligand capping.

Ligand exchange leads to smaller particles that can be applied to biosensing applications but entail a certain amount of loss of QD fluorescence. Alternatively, ligand capping coats the QDs with its surrounding surface groups, which leads to a larger hydrodynamic diameter but also the retention of its unique photophysical properties.<sup>15</sup> QDs coated by this technique can be applied to various diagnostic applications determined by their eventual size.

We demonstrate the application of polyhedral oligomeric silsesquioxane (POSS) as a novel surface coating for QDs. POSS is a cyclical silsesquioxane with a stoichiometric formula  $(\text{SiO}_{1.5})_8$ <sup>8</sup> and is the smallest of the silica nanoparticles with a size of 1.5 nm<sup>16</sup> (Figure 1). We have previously integrated POSS as a nanocomposite into a synthetic polymer polycarbonate urea urethane and used it for biomedical tissue engineering applications, such as vascular grafts, heart valves, nerve grafts<sup>15,17–26</sup> and more recently as a nasolacrimal duct and a tracheal graft, which have successfully been implanted into patients. POSS imparts properties of antithrombogenicity, biocompatibility, non-immunogenicity, and increased surface area to promote endothelialization. We have also used the emulsion form of this novel nanocomposite polymer to coat QDs.<sup>27</sup> POSS-PCU emulsion-coated QDs were biocompatible and more photostable than mercaptoundecanoic acid (MUA)-coated QDs but have a hydrodynamic diameter of ~33 nm. In this paper, we describe the application of a novel POSS coating to mercaptosuccinic acid (MSA) and D-Cysteine stabilized CdTe core QDs synthesized by modification of a simple one pot aqueous synthesis as previously described.<sup>6,28</sup> MSA achieves dispersibility and pH stability while D-cysteine acts as an anti-oxidant and adds both  $\text{NH}_2$  and  $-\text{COOH}$  groups for biofunctionalization. POSS imparts properties of colloidal stability, photostability, and amphiphilicity, allowing high intracellular uptake and lower concentrations of the QDs to be used for overall enhanced biocompatibility.

## Materials and methods

### Materials

Sodium borohydride ( $\text{NaBH}_4$ , 98%), sodium tellurite ( $\text{Na}_2\text{TeO}_3$ , 99.8%), cadmium chloride ( $\text{CdCl}_2$ ), MSA, D-cysteine (99.5%) and mercaptopropylisobutyl-POSS (M-POSS) were purchased from Sigma-Aldrich Chemicals (St Louis, MO). All chemicals were used as obtained without further purification. Dulbecco's modified eagle's medium (DMEM + 4.5 g/l glucose), fetal bovine serum (FBS) and penicillin/streptomycin, Trypsin/EDTA, and phosphate-buffered saline (PBS) were purchased from GIBCO/Invitrogen (UK).

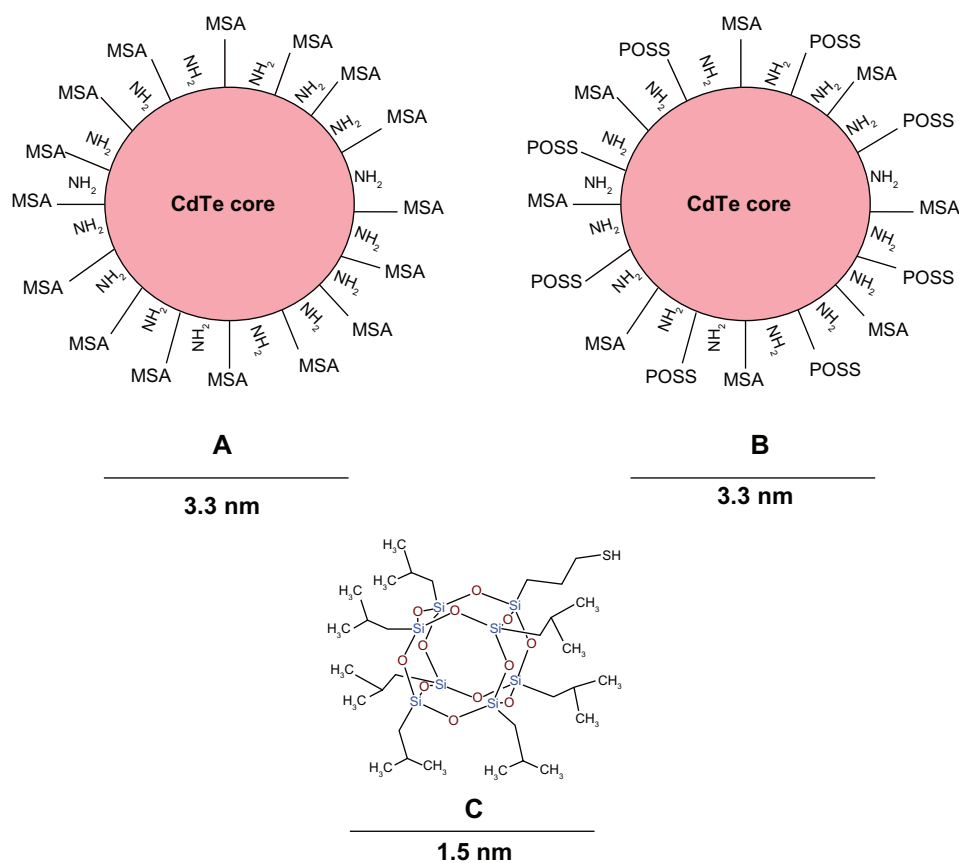


**Figure 1** Structure of QDs and M-POSS.

**Notes:** (A) MSA-QDs; (B) POSS-QDs; (C) M-POSS. MSA-QDs have ample surface COOH groups to allow solubility and stability. POSS-QDs have both hydrophobic and hydrophilic surface groups, giving them amphiphilic properties. Structure of M-POSS (C) shows a caged structure with predominant Si-O-Si and surface Si-C bonds. R groups promote solubility in organic solvents and thiol (-SH) group binds to QD core metal surface.

**Abbreviations:** QD, quantum dots; M-POSS, mercaptopropylisobutyl-polyhedral oligomeric silsesquioxane; MSA-QDs, mercaptosuccinic acid quantum dots; POSS-QDs, polyhedral oligomeric silsesquioxane quantum dots.

CellTitre-Blue® viability assay was purchased from Promega (Madison, WI, USA).

## Synthesis and coating of CdTe QDs

Briefly, borate-citrate acid-buffer solution was prepared using 15 mM sodium borate ( $\text{Na}_2\text{B}_4\text{O}_7$ ) and 15 mM citric acid and then pH adjusted with 1 M HCL or 1 M NaOH. The precursor solution was prepared using cadmium chloride ( $\text{CdCl}_2$ , 1 mM) and sodium tellurite ( $\text{Na}_2\text{TeO}_3$ , 0.25 mM), to which 0.1 mM of thiolated D-cysteine and 1 mM MSA was added. The materials were mixed in a single-necked flask immersed in ice and containing 50 mL of the buffer solution. After 5 minutes of vigorous stirring, 20 mg of sodium borohydride ( $\text{NaBH}_4$ ) powder was added, and the reaction was allowed to proceed for another 5 minutes before attaching the flask to a condenser and refluxing at  $100^\circ\text{C}$  under open-air conditions for approximately 6 hours. The emission color of the QDs could be controlled by altering reflux time. The QDs were purified from the suspension by centrifugation with an

equal volume of ethanol for 20 mins. The QDs obtained were MSA/D-cysteine-coated and referred to as MSA-QDs.

## Synthesis of POSS-coated CdTe QDs

Mercaptopropylisobutyl-POSS was first dissolved in tetrahydrofuran (THF) and then added to the precursor solution at a concentration of 0.1 mM along with 0.1 mM of D-cysteine and 1 mM solution of MSA. The solution was refluxed for the same period of time as the MSA-QDs. The QDs were purified with centrifugation with an equal volume of THF. The POSS/MSA/D-cysteine-coated QDs obtained were referred to as POSS-QDs. The final QD concentrations were calculated from the dry weight, and the QDs were suspended in PBS.

## Characterization studies

Photoluminescence spectra were obtained using a fluorescence emission spectroscopy USB 2000+ (Ocean Optics, Dunedin, FL) using a quartz cuvette with a 1 cm path

length and an aqueous solvent (deionized water or PBS) as a reference. QD samples were illuminated with a LED beam at 375 nm. Photostability of POSS and MSA QDs was assessed by exposing equal concentrations of QDs to continuous UV excitation at 375 nm for 2 hours, and emission intensity was recorded at sequential intervals. The emission intensities were normalized before comparison. The shape and size of the different QDs cores were assessed using transmission electron microscopy. A drop of QD samples was mounted on to a Piloform (TAAB)-coated G300HS copper electron microscopy grid (Gilder) and allowed to air dry. The grids were examined with a CM120 (Philips) transmission electron microscope at  $3.0 \times 10^5$  magnification. Fourier transform infrared spectra were obtained on a Jasco FT/IR 4200 spectrometer equipped with a diamond attenuated total reflectance accessory (Diamond MIRacle ATR, Pike Technologies, US). Spectra were produced from an average of 20 scans at  $4 \text{ cm}^{-1}$  resolution over a range of  $600 \text{ cm}^{-1}$  to  $4000 \text{ cm}^{-1}$  wavenumbers. For POSS and MSA-QDs, aqueous samples were run against a background generated from PBS solution. Dry MSA powder and M-POSS were run again against a background of air.

## Cell culture

Hep G2 cells were supplied at passage number 50 from the Liver Group at the Centre for Hepatology, Department of Medicine, Royal Free Hospital and Medical School, University College London. Once received, the media was changed to Dulbecco's modified eagle's medium (DMEM + 4.5 g/l glucose) and supplemented with fetal bovine serum (FBS, 10%) and penicillin/streptomycin (1%), which was then replaced a few times during a period of 1 week to 10 days. Part of the supply was cryopreserved for future use, and the rest was maintained ready for use as needed. The cells were seeded into flasks and cultured at  $37^\circ\text{C}$  and 5%  $\text{CO}_2$  under aseptic conditions. Cells were grown to 90% confluence before being used for routine passaging and in vitro toxicity experiments.

## Cell viability studies

Serial dilutions (0, 1.5, 5, 10, and 15  $\mu\text{g}/\text{mL}$ ) of  $\text{CdCl}_2$ ,  $\text{Na}_2\text{TeO}_3$ , and different QDs were prepared using PBS and media, whereby the volume of DMEM was kept constant. HepG2 cells were seeded into 96-well plates at a density of  $2 \times 10^4$  cells per well, and allowed to settle for 24 hours at  $37^\circ\text{C}$  in an incubator with 5%  $\text{CO}_2$ . After this period, the media was removed. The cells were thoroughly washed

with PBS and then exposed to serial dilutions of the  $\text{CdCl}_2$ ,  $\text{Na}_2\text{TeO}_3$  and three different types of QDs, and then incubated at  $37^\circ\text{C}$  in 5%  $\text{CO}_2$  for 1 and 24 hours. After this period, the cells were thoroughly washed with PBS, and the QD dilutions were replaced with DMEM. Twenty  $\mu\text{l}$  of the CellTitre-Blue<sup>®</sup> dye was then added to each well and incubated for further 4 hours at  $37^\circ\text{C}$  in 5%  $\text{CO}_2$ . All tests were conducted in triplicate. Cells not exposed to any QD dilution ( $0 \mu\text{g}/100 \mu\text{l}$ ) served as a negative control and those exposed to ionized  $\text{Cd}^{+2}$  and  $\text{Te}^{-2}$  served as positive controls for toxicity.

## Confocal microscopy to assess cell morphology and QD stability

For confocal microscopy, cells were plated in flat-bottomed glass 96-well plates and exposed to QD dilutions as above. They were washed with PBS, fixed with glutaraldehyde, and examined using an EC-1 confocal microscope from Nikon. Each respective image was optimized by averaging 10 scans per image.

## Statistical analysis

Statistical analysis was performed using Prism software and one-way ANOVA with the Dunnett and Bonferroni multiple comparison test and paired *t* test.

## Results Synthesis

The CdTe core QDs were synthesized by a previously described one pot aqueous method based on the reaction between  $\text{CdCl}_2$  and  $\text{Na}_2\text{TeO}_3$  in a borate-citrate buffer.<sup>6,27</sup> Bao et al were the first to describe a one pot aqueous synthesis of L-cysteine capped CdTe nanocrystals using sodium tellurite as a Tellurium source.<sup>28</sup> The same group adapted this technique to demonstrate the synthesis of highly luminescent MSA capped CdTe QDs.<sup>6</sup> We made minor modifications to this protocol with respect to the coating materials to yield two different types of QDs coated with MSA and D-cysteine (referred to as MSA-QDs) and mercaptopropylisobutyl-POSS (M-POSS), MSA and D-cysteine (referred to as POSS-QDs) (Figure 1).

The synthesis of MSA-QDs involved preparing a precursor solution by mixing cadmium chloride, sodium tellurite, MSA, and D-cysteine in a borate citrate buffer. When sodium borohydride was added, the color of the growth solution instantly turned a light green. On heating the mixture at  $100^\circ\text{C}$  for 1 hour, the color darkened to a deep green and eventually to brown at the end of 6 hours. By altering the



reflux time, QD emission of the desired wavelength could be achieved with bluish fluorescence (450 nm) at the end of 1 h, yellow (550 nm) at 4 h and red (635 nm) at 6 h. Reflux times of greater than 6 h led to the solution becoming unstable with evidence of aggregation and loss of fluorescence. It is likely that prolonged heating may lead to breakdown of the thiol groups to form a CdS shell initially followed by oxidation of the cysteine residues to cystine with formation of a disulphide bond. MSA QDs were purified after centrifugation with equal amounts of isopropanol and resuspended readily in PBS. However, the MSA-QDs lacked colloidal stability as they fell out of solution under prolonged standing in refrigeration within a few days.

For the synthesis of POSS-QDs, Mercaptopropylisobutyl-POSS (M-POSS) was dissolved in tetrahydrofuran to make a 0.1 mM solution. This was added to the precursor solution, including cadmium chloride, sodium tellurite, MSA, and D-cysteine in 50 mL of buffer solution in a single-necked flask immersed in ice and subjected to vigorous stirring in a homogenizer. The initial temperature of the flask was kept low to prevent initiation of the reaction prior to addition of all the materials. As an organic solvent was added to the aqueous solution, vigorous stirring was required to form a homogenous mixture. After addition of the reducing agent, sodium borohydride, the reaction proceeded as previously. At the end of 6 hours, a brown colored solution was obtained with some precipitates of free POSS present in the base of the flask. POSS-QDs emitting at 630 nm were purified with centrifugation with an equal amount of tetrahydrofuran to remove any unreacted M-POSS. They readily suspended in PBS and remained colloidal stable on prolonged standing

at 4°C in refrigeration for months. Successful coating of the QDs was later confirmed by Fourier transform infrared spectroscopy (FTIR) analysis.

## Characterization studies

The core diameter, shape, and degree of dispersion of the QDs were assessed using transmission electron microscopy (Figure 2). Both QDs were spherical in shape and had a mean core diameter of 3.3 nm. MSA-QDs appeared to be marginally better dispersed than POSS-QDs. Photoluminescence studies showed that MSA-QDs emitted at 635 nm, whereas POSS-QDs showed a marginal blue shift in emission at 630 nm (Figure 3).

The FTIR spectra of dry MSA powder, MSA-QDs, POSS-QDs, and M POSS are shown in Figure 4. Both MSA and POSS-QDs show prominent peaks at 1565  $\text{cm}^{-1}$  and 1402  $\text{cm}^{-1}$ , which correspond to strong asymmetric and symmetric stretching vibrations of amino acid cysteine, respectively. The peak at 1402  $\text{cm}^{-1}$  (MSA-QDs) and 1403  $\text{cm}^{-1}$  (POSS-QDs) is strongest as it also receives some contribution from weak deformation of O-H groups from the MSA (1418  $\text{cm}^{-1}$ ). MSA-QDs show a slight shift in the peak at 1646  $\text{cm}^{-1}$  from 1689  $\text{cm}^{-1}$  in the MSA powder caused by carbonyl stretching vibrations, indicating that MSA has bonded to the QD surface. POSS-QDs show a new peak at 1043  $\text{cm}^{-1}$  from variable strong stretching vibrations of the Si-O-Si bonds in the POSS nanocages. The FTIR spectrum of M-POSS indicates a strong peak at 1080  $\text{cm}^{-1}$  from the Si-O-Si bonding of the POSS nanocages. The shift in this peak from 1080  $\text{cm}^{-1}$  in M-POSS to 1043  $\text{cm}^{-1}$  in POSS-QDs indicates that the

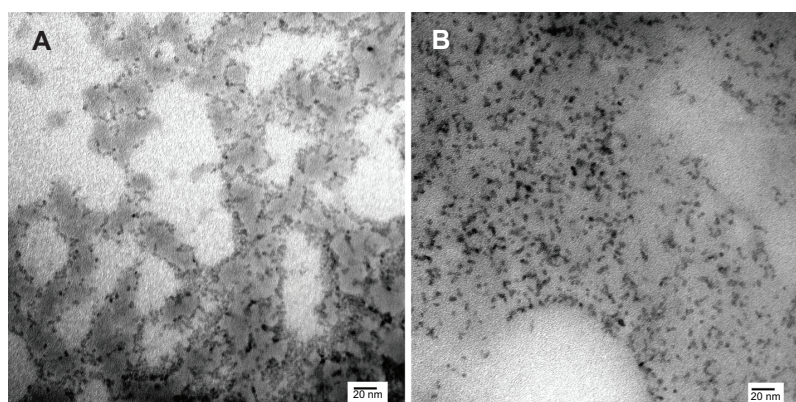


**Figure 2** Transmission electron microscopy.

**Notes:** (A) POSS-QDs; (B) MSA-QDs. The core sizes of CdTe in (A) and (B) are 3.3 nm. Both QDs (A and B) were well dispersed, although some darker areas in A may reflect free POSS. Scale bars represent 20 nm. Magnification  $\times 300,000$ .

**Abbreviations:** POSS-QDs, polyhedral oligomeric silsesquioxane quantum dots; MSA-QDs, mercaptosuccinic acid quantum dots; QDs, quantum dots; POSS, polyhedral oligomeric silsesquioxane.

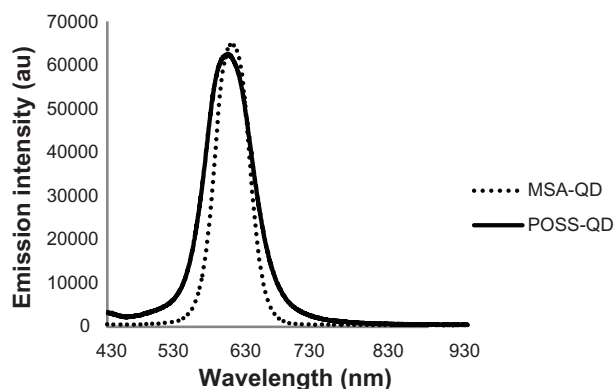


**Figure 3** Fluorescence emission spectra of POSS and MSA-QDs.

**Notes:** POSS-QDs emit at 630 nm and MSA-QDs at 635 nm. There is no significant difference in the peak emission wavelength of both QDs, although POSS-QDs have a slightly broader FWHM compared to MSA-QDs.

**Abbreviations:** POSS, polyhedral oligomeric silsesquioxane; MSA-QDs, mercaptosuccinic acid quantum dots; POSS-QDs, polyhedral oligomeric silsesquioxane quantum dots; QDs, quantum dots.

POSS has bonded to the QD surface. Both POSS and MSA QDs have cysteine residues and MSA groups, which relate to the similarity of their FTIR spectra, except for the POSS peak that occurs at  $1043\text{ cm}^{-1}$  and a slightly more prominent broad peak at  $1154\text{ cm}^{-1}$  in POSS-QDs caused by skeletal vibrations of alkyl C-C groups from the isobutyl alkyl groups on the POSS nanocages.

POSS-QDs were more resistant to photo-oxidation on exposure to high degrees of UV illumination compared to MSA-QDs ( $P$ -value  $< 0.05$ ) (Figure 5). Although both types of QDs photo-degraded over the period of exposure, the rate of decline of the emission intensity of POSS-QDs was considerably less than MSA-QDs. POSS-QDs remained photostable for the initial 20 minutes of UV exposure and lost 25% of their emission intensity over a period of 1 hour. In comparison, MSA-QDs lost  $>25\%$  of their emission intensity in the first 20 minutes and  $>50\%$  after the first hour of exposure.

## Cell viability studies

In vitro toxicity of individual heavy metals of  $\text{CdCl}_2$  and  $\text{Na}_2\text{TeO}_3$  was carried out to establish the toxicity of free divalent  $\text{Cd}^{+2}$  and  $\text{Te}^{-2}$  ions, which was compared with toxicity of the two different types of QDs. Both tellurium and cadmium individually demonstrated significant time and concentration dependent cytotoxicity (Figure 6). Cadmium toxicity was more pronounced even at low concentration of  $1.25\text{ }\mu\text{g/mL}$  at 1 hour ( $P$ -value  $< 0.01$ ). At 24 h exposure, all concentrations of cadmium showed less than 10% cell viability versus tellurium, which showed a similar effect at  $5\text{ }\mu\text{g/mL}$ .

Hep G2 cells exposed to MSA and POSS-QDs showed no significant evidence of toxicity at concentrations of  $2.5\text{ }\mu\text{g/mL}$  at both 1 h and 24 h of exposure (Figure 7). At the end of 1 h, the first signs of toxicity appeared at  $5\text{ }\mu\text{g/mL}$  even though both POSS and MSA-QDs maintained greater than 85% cell viability at all concentrations up to  $15\text{ }\mu\text{g/mL}$ . There was no significant difference in toxicity between the two QDs at 1 h of exposure. At 24 h, POSS-QDs showed significantly reduced cell viability at  $5\text{ }\mu\text{g/mL}$  compared to MSA-QDs ( $P$ -value  $< 0.01$ ) even though they maintained a cell viability of  $\sim 90\%$ . The slightly greater cell viability of both POSS and MSA QDs at 24 h compared to 1 h, at  $5\text{ }\mu\text{g/mL}$  indicates that both QDs do not affect the multiplication potential of cells at this concentration. At higher concentrations of  $\geq 10\text{ }\mu\text{g/mL}$  both POSS and MSA QDs were toxic at 24 h ( $P$ -value  $< 0.01$ ). Although there was no significant difference in cell viability between the two QDs at higher concentrations, MSA-QDs showed marginally higher cell viability ( $\sim 70\%$ ) compared to POSS-QDs ( $\sim 65\%$ ) at the highest concentration of  $15\text{ }\mu\text{g/mL}$  (Figure 7).

## Cellular morphology

Confocal images of HepG2 cells exposed to the highest QD concentration ( $15\text{ }\mu\text{g/mL}$ ) were taken to demonstrate changes in cell morphology and uptake of QDs after 1 and 24 hours of exposure (Figures 8 and 9, respectively). At 1 hour post incubation, there was no visible difference in morphology between cells exposed to POSS and MSA-QDs. However, at 24 hours post incubation, cells exposed to  $\text{Cd}^{+2}$  displayed marked evidence of cell death with loss of cellular architecture and evidence of cellular break down. POSS and MSA QDs exhibited distinctly higher cell numbers and intracellular fluorescence. The fluorescence of POSS-QDs was more predominant at both 1 and 24 hours.

## Discussion

The synthesis of highly luminescent MSA and L-cysteine capped CdTe QDs has previously been described.<sup>6,28</sup> We modified the same technique to apply a POSS coating and replaced the conventionally used L-cysteine with its enantiomer D-cysteine. L-cysteine is a small amino acid present in the human body and susceptible to degradation by physiological proteases. As D-cysteine is resistant to such degradation,<sup>29</sup> we hypothesized that it would provide superior protection to the QD core in a biological environment while retaining the advantages of the L-cysteine molecule. D-cysteine has both  $\text{NH}_2$  and  $\text{COOH}$  groups, which solubilize the QDs and provide free reactive groups for the attachment of biomolecules.

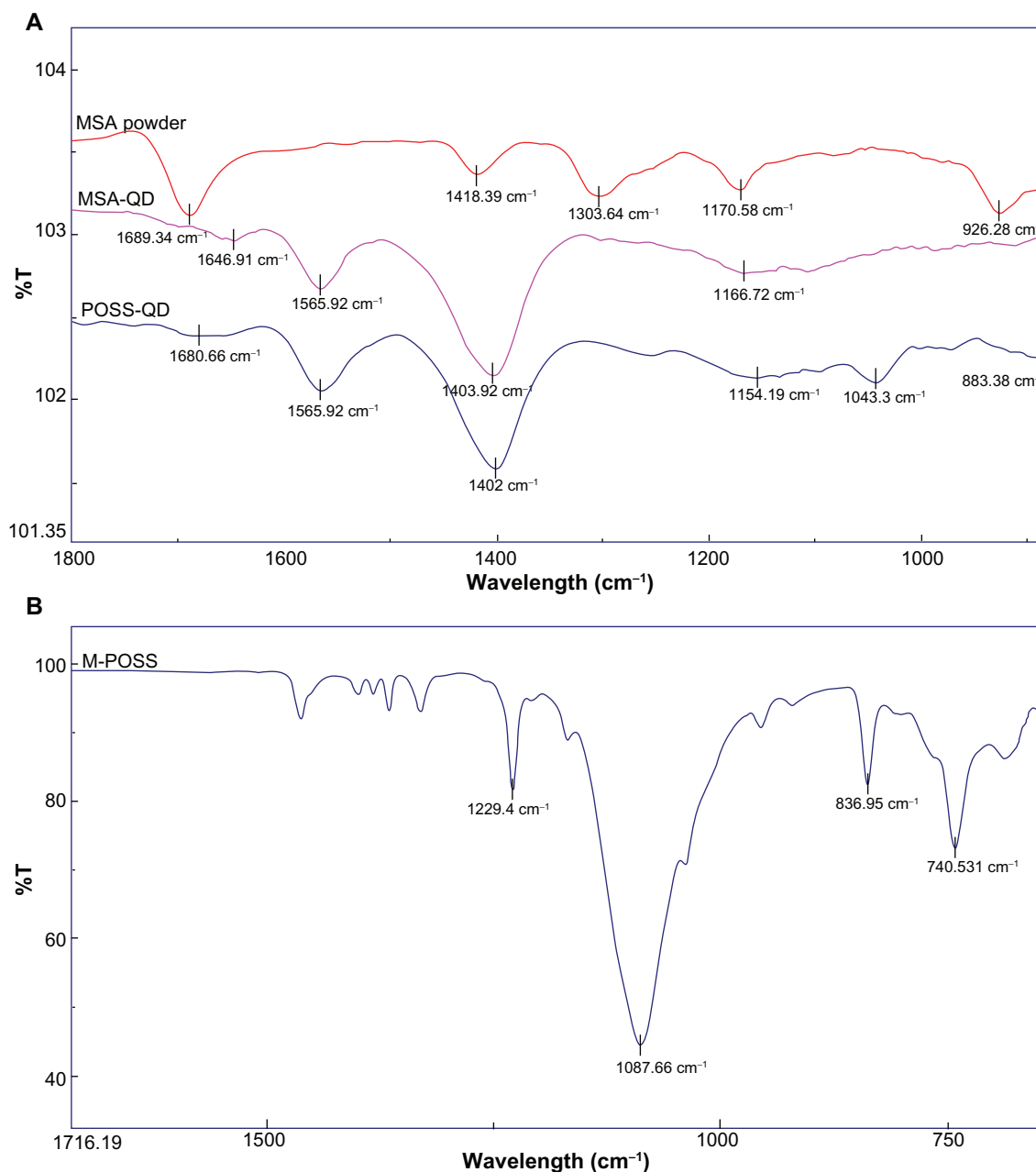


**Figure 4** FTIR spectra of dry MSA powder, MSA-QDs, POSS-QDs and M-POSS.

**Notes:** (A) POSS and MSA-QDs show common peaks at 1402  $\text{cm}^{-1}$  and 1565  $\text{cm}^{-1}$  from strong symmetric and asymmetric vibrations of the amino acid cysteine. However, POSS-QDs show a new peak at 1043  $\text{cm}^{-1}$  that corresponds to stretching vibrations from Si-O-Si bonds in POSS; (B) M-POSS demonstrates a prominent peak at 1087  $\text{cm}^{-1}$  from Si-O-Si bonds that shifts to a 1043  $\text{cm}^{-1}$  on the POSS-QDs indicating that POSS has bonded to the QD surface.

**Abbreviations:** FTIR, Fourier transform infrared spectroscopy; MSA, mercaptosuccinic acid; MSA-QDs, mercaptosuccinic acid quantum dots; POSS-QDs, polyhedral oligomeric silsesquioxane quantum dots; M-POSS, Mercaptopropylisobutyl-polyhedral oligomeric silsesquioxane; POSS, polyhedral oligomeric silsesquioxane; QDs, quantum dots.

We did not investigate the effects of pH, molar ratios, and reaction temperature on QD synthesis. Our aim was to apply a novel POSS coating to MSA and D-cysteine stabilized CdTe core QDs and establish its effect on their eventual biocompatibility and QD photophysical properties.

Both POSS and MSA-QDs were monodispersed with a core diameter of 3.3 nm on a transmission electron microscopy (TEM) although MSA-QDs showed marginally

better dispersibility than POSS-QDs (Figure 2). TEM does not assess the hydrodynamic diameter of QDs as the soft organic coating is not electron dense and therefore invisible. The MSA-QDs are compact as both MSA and cysteine residues are fairly small. Previous DLS studies to evaluate the hydrodynamic diameter of L-cysteine capped CdTe/ZnTe QDs suggested that cysteine adds 0.3–0.5 nm to the original QD size,<sup>30</sup> keeping the overall size of the QDs fairly small. POSS

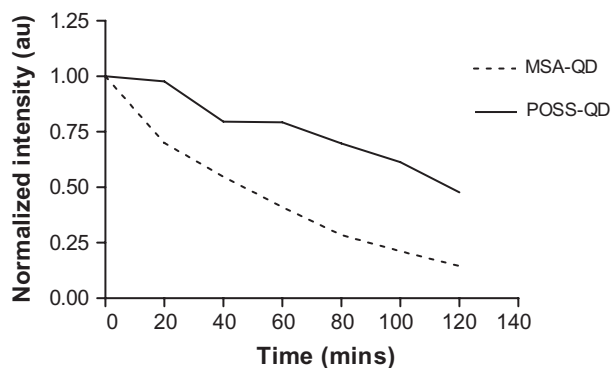


**Figure 5** Photostability of POSS and MSA-QDs.

**Notes:** On exposure to UV illumination for 2 hours, POSS-QDs undergo photo-oxidation at a much slower rate showing significantly enhanced photostability compared to MSA-QDs.  $P$  value < 0.05.

**Abbreviations:** POSS, polyhedral oligomeric silsesquioxane; MSA-QDs, mercaptosuccinic acid quantum dots; POSS-QDs, polyhedral oligomeric silsesquioxane quantum dots.

is a small molecule with a diameter of only 1.5 nm including R groups. We speculate that because it replaces some of the MSA groups on the QDs surface, it does not significantly alter the overall hydrodynamic (HD) diameter compared to MSA QDs. The MSA coating provides 2 carbonyl groups that

enhance miscibility and dispersibility as evident on TEM. However, after prolonged standing, the MSA-QDs appear to fall out of solution as compared to the POSS-QDs that maintain dispersibility and colloidal stability for prolonged periods of time.

POSS-QDs have all three residues on their surface, including D-cysteine, MSA, and M-POSS. The ratio of D-cysteine and POSS is very low compared to MSA (1:1:10, respectively), which serves as the main stabilizing agent. The POSS cage is ~1.5 nm in diameter,<sup>16</sup> and on its own is extremely hydrophobic. In the presence of MSA and D-Cysteine, it imparts amphiphilic properties to the QD. POSS is a robust molecule that has been incorporated into various polymers to protect the underlying surface from the effects of oxygen plasma.<sup>16</sup> It is likely that the POSS coating confers prolonged colloidal stability through reducing QD aggregation and maximally shielding the core from the oxidative effects of air and light.

Photoluminescence studies showed that MSA-QDs emitted at 635 nm while POSS-QDs showed a marginal blue shift in emission at 630 nm (Figure 3). A possible explana-

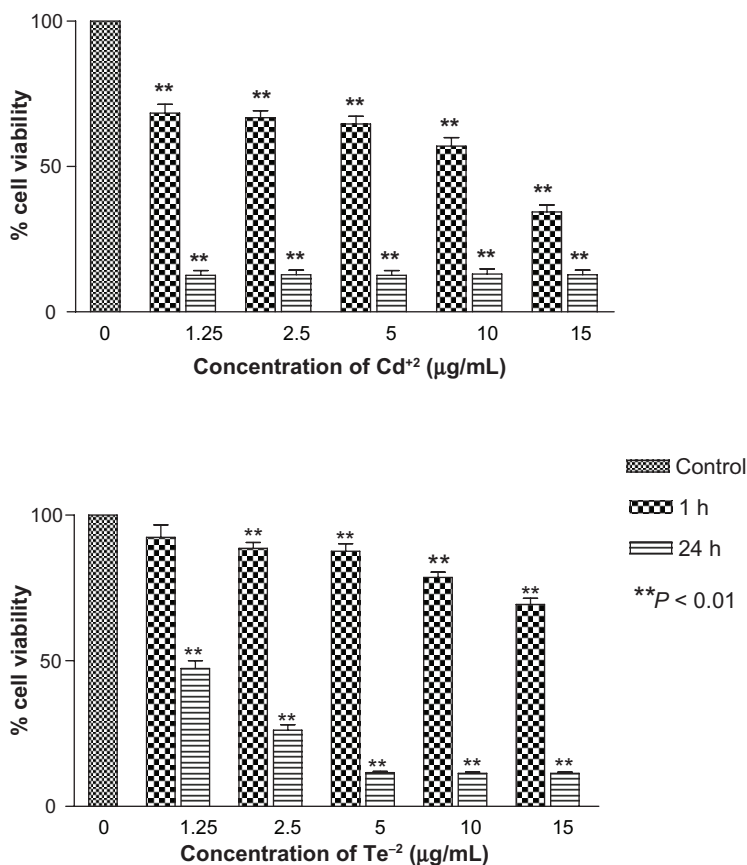


**Figure 6** In vitro toxicity of ionized Cd<sup>2+</sup> and Te<sup>2-</sup> to Hep G2 cells.

**Notes:** Both metals have profound toxicities, with cadmium being toxic at all concentrations at 1 and 24 hours compared with tellurium, which is toxic at all concentrations except 1.25 µg/mL at 1 hour.  $**P < 0.01$ .



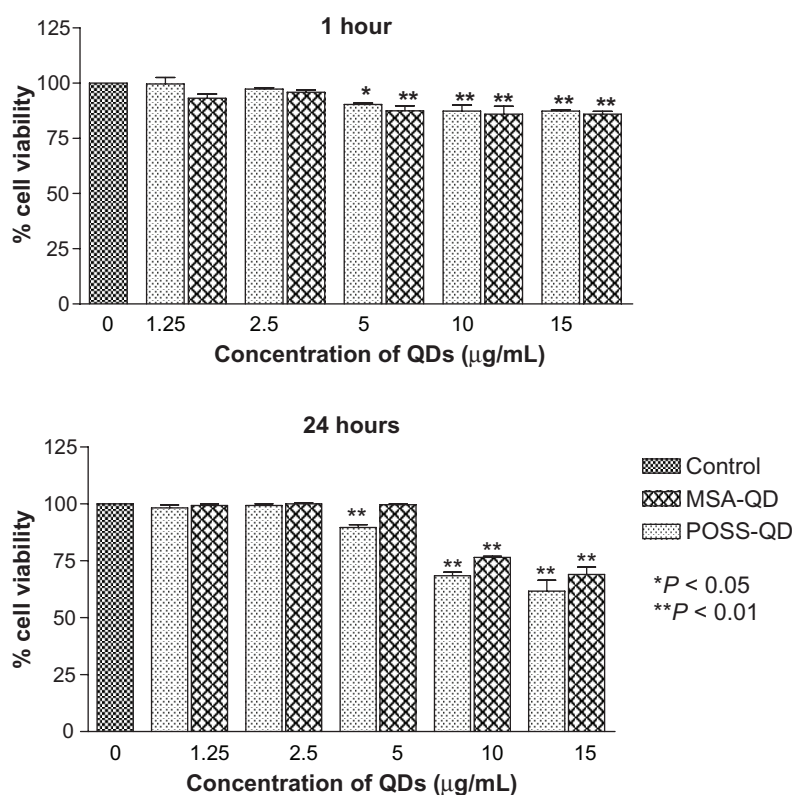


**Figure 7** In vitro toxicity of POSS and MSA-QDs to Hep G2 cells.

**Notes:** Different concentrations of QDs were compared to the control group. Both POSS and MSA-QDs are biocompatible at 2.5 µg/mL at 1 and 24 hours. POSS-QDs show lower cell viability at 5 µg/mL at 24 hours compared to MSA-QDs, although there is no significant difference in cell viability between the 2 QDs at higher concentrations of 10 and 15 µg/mL. \*P < 0.05; \*\*P < 0.01.

**Abbreviations:** POSS, polyhedral oligomeric silsesquioxane; MSA-QDs, mercaptosuccinic acid quantum dots; QDs, quantum dots; POSS-QDs, polyhedral oligomeric silsesquioxane quantum dots.

tion of this effect may be the initial loss of few atoms from the QD surface during the process of ligand exchange as M-POSS replaces some MSA groups on the QD surface. This phenomenon is a well-established sequel of ligand exchange reaction, which is one of the mechanisms of coating QDs for aqueous solubility.<sup>15</sup> Most commercially available QDs have a core/shell structure with a surface coating for solubility. Although both POSS and MSA-QDs emit at red wavelengths, they are core QDs without a shell and with small molecule thiol surface coating, which keeps the overall size of the QDs smaller than core/shell or core/shell/shell structures. The small size is a beneficial feature, particularly for various biosensing applications that track the movement of individual molecules within cells. Moreover, smaller particles are less likely to be taken up and accumulate in the reticuloendothelial system and more likely to be excreted by the kidneys.<sup>13</sup> Studies have proven the direct association between long-term retention of large cadmium-based QDs in the liver and its associated toxicity.<sup>31</sup>

The photostability of both POSS and MSA-QDs was assessed using prolonged UV excitation using a high powered

lamp. POSS-QDs have significantly higher photostability after two hours of UV exposure (Figure 5). Although the degree of UV excitation used in this experiment was very high and unlikely to be replicated in a biological environment, it gave an indication of the photochemical stability of the different coatings in extreme oxidative environments. The relative protective effect of POSS in retarding UV induced photooxidation may be related to the inherent structure of the POSS molecule. The Si-O bonds in the POSS structure are most resistant to breakdown compared to the Si-C bonds. In extreme exposures to oxidative environments, all the bonds may break down except the Si-O bond, which may form SiO<sub>2</sub> and protect the underlying QD from the effects of UV. This phenomenon has been demonstrated when POSS has been integrated as a nanocomposite in polymers for surface coatings<sup>32</sup> and exposed to oxygen plasma. The SiO<sub>2</sub> layer may prevent the loss of excitons, leading to enhanced photostability of POSS-QDs.

Previous studies have demonstrated that a QD concentration of only 10 µg/mL was toxic to HepG2 cells.<sup>33-35</sup> The cytotoxicity of cadmium based core QDs lacking a ZnS shell

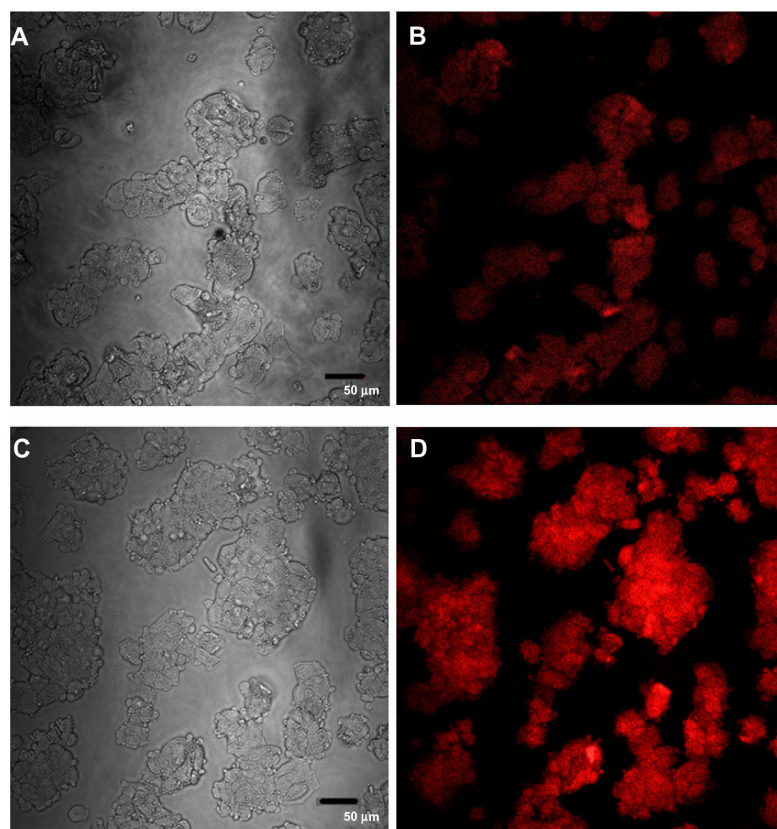


**Figure 8** Confocal images of HepG2 cells incubated with QDs for 1 hour. **(A)** Differential interference contrast (DIC) image of cells incubated with MSA-QDs; **(B)** Fluorescent image of A; **(C)** DIC image of cells incubated with POSS-QDs; **(D)** Fluorescence image of C; POSS-QDs **(D)** appear more brightly fluorescent than MSA-QDs **(B)** at 1 hour.

**Notes:** The images are pseudo-colored. The scale bar is set to 50  $\mu\text{m}$ .

**Abbreviations:** QD, quantum dots; MSA-QDs, mercaptosuccinic acid quantum dots; POSS-QDs, polyhedral oligomeric silsesquioxane quantum dots.

has also been well established.<sup>36</sup> Because our QDs lacked a ZnS coat, we used 15  $\mu\text{g/mL}$  as the highest concentration to evaluate cytotoxicity. It can be assumed that a surface coating that nullifies or reduces QD core toxicity would yield much greater biocompatibility with core/shell QDs. Core QDs may also be a more sensitive tool to assess QD toxicity because the slightest instability or breakdown of the surface coating would lead to an immediate oxidation of the core, manifesting as enhanced toxicity or photochemical instability.

The marginally lower cell viability on exposure to POSS-QDs compared to MSA QDs (Figure 7) can be explained by the possibility that POSS-QDs are rapidly taken up by the cells as evidenced by the brighter photoluminescence of cells on confocal microscopy at both 1 and 24 hr (Figures 8 and 9). The ideal method of confirming a high intracellular uptake would be a TEM that would allow counting the number of particles within the cells or determining the intracellular cadmium content through inductively coupled plasma mass spectroscopy of cell lysates. Quantification of fluorescence may not be ideal in this situation as the POSS-QDs are significantly more photostable than MSA-QDs,

and the brighter fluorescence may just be an indicator of photostability. However, we speculate that POSS-QDs have a surface coating with both hydrophobic and hydrophilic moieties, giving them amphiphilic properties, which may allow rapid intracellular uptake across the lipophilic cell membranes leading to slightly higher toxicity compared to MSA-QDs at concentrations  $\geq 5 \mu\text{g/mL}$  at 24 h. In a recent report, Su et al<sup>37</sup> demonstrated that the cytotoxicity of QDs cannot be solely attributed to the release of free  $\text{Cd}^{2+}$  ions but is actually determined by the number of QDs ingested by the cell. Our results correlate with those of previous studies showing concentration and time dependent toxicity of QDs.<sup>12,14,35</sup>

At one hour post-incubation, both POSS and MSA QDs were taken up by the cells and localized to the cytoplasm. The main mechanism of intracellular delivery of QDs is endocytic uptake, which is likely to be the mechanism by which both QDs were taken up. However, this method is very non-specific and leads to aggregation of QDs in vesicles and a non-uniform cytoplasmic distribution. QD sequestration into vesicles may also be a barrier to various clinical

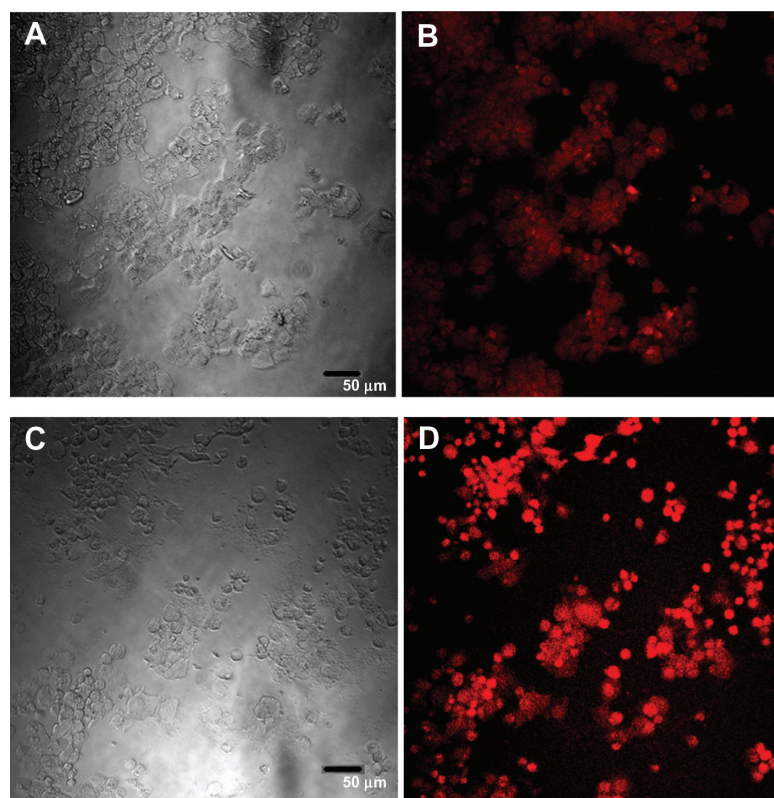


**Figure 9** Confocal images of HepG2 cells incubated with QDs for 24 hours.

**Notes:** (A) differential interference contrast (DIC) image of cells exposed to MSA-QDs; (B) Fluorescent image of A; (C) DIC image of cells exposed to POSS-QDs (D) Fluorescence image of C. Both POSS and MSA-QDs maintain high cellular numbers and intracellular fluorescence indicating uptake of QDs. POSS-QDs (D) appear brighter than MSA-QDs (C).  
**Abbreviations:** QD, quantum dots; MSA-QDs, mercaptosuccinic acid quantum dots; POSS-QDs, polyhedral oligomeric silsesquioxane quantum dots; POSS, polyhedral oligomeric silsesquioxane.

applications, eg, QD-bioconjugates as drug-delivery systems, since intracellular delivery requires the QD-drug complex to be freely available for interactions. Trapped QDs, however, cannot reach the intended target and thus render the system futile. Other methods of QD uptake by cells include techniques such as microporation and microinjection of QDs<sup>38,39</sup> into individual cells, which appears to be the only means of homogeneous intracellular QD delivery to date. However, the major drawback of this technique is the single cell approach, which makes it a laborious process and thus precludes large-scale applications.

A major finding of our study was that the degree of QD fluorescence in cells was considerably higher for the POSS-QDs compared to the MSA-QDs, particularly at 1 h post incubation. It is possible that the mechanism of QD uptake for POSS-QDs differs from MSA QDs such that the former are rapidly taken up by pathways other than non-specific endocytosis, leading to increased QD concentration within the cells and higher intracellular fluorescence. It has been previously demonstrated that QD uptake by cells can be enhanced by conjugating the QDs to cationic lipids or

peptides<sup>39-42</sup> or amphiphilic proteins.<sup>43</sup> Cationic lipid-capped QD delivery into tumor cells was successfully demonstrated by Voura et al<sup>40</sup> as was peptide-mediated delivery of QDs into Chinese hamster ovarian cells.<sup>42</sup> Cationic POSS conjugated to BODIPY was seen to be taken up by cells with a uniform cytoplasmic distribution.<sup>44</sup> Although the M-POSS used to coat our QDs is not the cationic form, it is likely that the amphiphilicity that it imparts to the QD structure has a role in its increased intracellular uptake across the lipophilic cell membranes. At 24 hours post incubation, a significant rise in fluorescence of both POSS and MSA QDs could be detected due to increased intracellular uptake over time. However, POSS-QDs fluoresced more brightly compared to MSA-QDs owing to their relatively higher photostability on exposure to oxidative environments.

Our study demonstrates the application of a novel POSS nanoparticle as coating for QDs for biological application. We used CdTe cored QDs without a ZnS shell. It has been established that a QD coating of a higher band gap material removes surface defects and retains excitons, thus leading to prolonged photostability, higher quantum yield, and



enhanced biocompatibility.<sup>45–48</sup> However, QD toxicity is not eliminated as ZnS-coated QDs do show concentration dependent increase in toxicity.<sup>38</sup> Aqueous solubility still requires further coating of the ZnS shell with materials such as MSA, PEG, dihydrolipoic acid, silica, dendrimers, amphiphilic polymers, phospholipids micelles, etc. for biological application.<sup>9,15,49,50</sup> This significantly increases the size of the coated QDs (15–100 nm), leading to problems of excretion and QD sequestration into the organs of the RES, apart from significant limitation to their biological applications. We used POSS, MSA and D-Cysteine to coat QDs in an attempt to achieve solubility with the MSA ligand, and biocompatibility and stability through the POSS coating while retaining the small QD size. Although the toxicity of POSS and MSA-QDs is comparable, POSS QDs show marginally lower cell viability compared to MSA-QDs at 5 µg/mL. This is unlikely to be caused by the surface coating itself as the biocompatibility of POSS has been well established. Furthermore, the enhanced photostability of the POSS-QDs compared to MSA-QDs indicates that the POSS coating adequately shields the core from the effects of photochemical oxidation. Therefore, the most likely explanation for this effect is the higher cellular uptake of POSS-QDs, which leads to reduced cell viability. This particular property, in addition to enhanced photostability, may allow lower concentrations of POSS-QDs to be used for various biological applications, such as long term in vitro and in vivo imaging applications like single particle tracking and stem cell tracking as well as various biosensing applications that rely on a small QD size.

## Conclusion

We have demonstrated that the novel POSS coating confers photostability, colloidal stability, and biocompatibility on MSA and D-cysteine stabilized CdTe core QDs. Although the biocompatibility of POSS-QDs is comparable to MSA-QDs, the POSS coating imparts amphiphilicity to the QD surface, allowing rapid intracellular uptake and brighter fluorescence, which eventually leads to lower concentrations of QDs required for use. POSS-QDs retain surface reactive groups for bioconjugation, which along with their small size, confers numerous advantages for use in various biomedical applications. The POSS molecule is known to confer anti-thrombogenic properties when incorporated in polymer nanocomposites for vascular grafts.<sup>26</sup> Few studies have examined the hemocompatibility of QDs, which is essential prior to any consideration for in vivo and clinical application. It is likely that the POSS coating may impart

similar properties to QDs, but further testing is required to establish this effect. Future experiments to investigate in vivo biodistribution and toxicity of POSS-coated QDs are now in progress to move them one step closer to clinical application.

## Acknowledgments

We would like to acknowledge the financial support of The Sebba Trust, UK for the development of QDs for detection of breast cancer and an MRC research grant on POSS-PCU.

## Disclosure

The authors report no conflicts of interest in this work.

## References

- Gao X, Chan WC, Nie S. Quantum-dot nanocrystals for ultrasensitive biological labeling and multicolor optical encoding. *J Biomed Opt.* 2002;7:532–537.
- Curtis A, Wilkinson C. Nanotechnology and approaches in biotechnology. *Trends Biotechnol.* 2001;19:97–101.
- Gref R, Minamitake Y, Peracchia MT, Trubetsky V, Torchilin V, Langer R. Biodegradable long-circulating polymeric nanospheres. *Science.* 1994;263:1600–1603.
- Weissleder R. A clearer vision for in vivo imaging. *Nat Biotechnol.* 2001;19:316–317.
- Frangioni JV. In vivo near-infrared fluorescence imaging. *Curr Opin Chem Biol.* 2003;7:626–634.
- Ying E, Li D, Guo S, Dong S, Wang J. Synthesis and bio-imaging application of highly luminescent mercaptosuccinic acid-coated CdTe nanocrystals. *PLoS One.* 2008;3:e2222.
- Bruchez M, Moronne M, Gin P, Weiss S, Alivisatos AP. Semiconductor nanocrystals as fluorescent biological labels. *Science.* 1998;281:2013–2016.
- Alivisatos AP. Semiconductor clusters, nanocrystals, and quantum dots. *Science.* 1996;271:933–937.
- Smith AM, Duan H, Rhyner MN, Ruan G, Nie S. A systematic examination of surface coatings on the optical and chemical properties of semiconductor quantum dots. *Phys Chem Chem Phys.* 2006;8:3895–3903.
- Anderson RE, Chan WCW. Systematic investigation of preparing biocompatible, single, and small ZnS-capped CdSe quantum dots with amphiphilic polymers. *ACS Nano.* 2008;2:1341–1352.
- Tsay JM, Pflughoefft M, Bentolila LA, Weiss S. Hybrid approach to the synthesis of highly luminescent CdTe/ZnS and CdHgTe/ZnS nanocrystals. *J Am Chem Soc.* 2004;126:1926–1927.
- Hardman R. A toxicologic review of quantum dots: toxicity depends on physicochemical and environmental factors. *Environ Health Perspect.* 2006;114:165–172.
- Choi HS, Ipe BI, Misra P, Lee JH, Bawendi MG, Frangioni JV. Tissue- and organ-selective biodistribution of NIR fluorescent quantum dots. *Nano Lett.* 2009;9:2354–2359.
- Shiohara A, Hoshino A, Hanaki K, Suzuki K, Yamamoto K. On the cytotoxicity caused by quantum dots. *Microbiol Immunol.* 2004;48:669–675.
- Hezinger AFE, Tessmar J, Gopferich A. Polymer coating of quantum dots: a powerful tool toward diagnostics and sensorics. *Biopharmaceutics.* 2008;68:138–152.
- Li GZ, Wang LC, Ni HL, Pittman CU. Polyhedral oligomeric silsesquioxane (POSS) polymers and copolymers: A review. *J Inorg Organomet Polym.* 2001;11:123–154.
- Ghanbari H, Kidane AG, Burriesci G, Ramesh B, Darbyshire A, Seifalian AM. The anti-calcification potential of a silsesquioxane nanocomposite polymer under in vitro conditions: potential material for synthetic leaflet heart valve. *Acta Biomater.* 2010;6:4249–4260.

18. Kannan RY, Sales KM, Salacinski HJ, Butler PE, Seifalian AM. Endothelialisation of poly (carbonate-siloxane-urea) urethane. *Med J Malaysia*. 2004;59 Suppl B:107–108.
19. Kannan RY, Sales KM, Salacinski HJ, Butler PE, Seifalian AM. Cytotoxicity analysis of poly (carbonate-siloxane-urea) urethane. *Med J Malaysia*. 2004;59 Suppl B:99–100.
20. Kannan RY, Salacinski HJ, Butler PE, Hamilton G, Seifalian AM. Current status of prosthetic bypass grafts: a review. *J Biomed Mater Res B Appl Biomater*. 2005;74:570–581.
21. Kannan RY, Salacinski HJ, Butler PE, Seifalian AM. Polyhedral oligomeric silsesquioxane nanocomposites: the next generation material for biomedical applications. *Acc Chem Res*. 2005;38:879–884.
22. Kannan RY, Salacinski HJ, Sales K, Butler P, Seifalian AM. The roles of tissue engineering and vascularization in the development of microvascular networks: a review. *Biomaterials*. 2005;26:1857–1875.
23. Kannan RY, Salacinski HJ, Sales KM, Butler PE, Seifalian AM. The endothelialization of polyhedral oligomeric silsesquioxane nanocomposites: an in vitro study. *Cell Biochem Biophys*. 2006;45:129–136.
24. Kannan RY, Salacinski HJ, Odlyha M, Butler PE, Seifalian AM. The degradative resistance of polyhedral oligomeric silsesquioxane nanocore integrated polyurethanes: an in vitro study. *Biomaterials*. 2006;27:1971–1979.
25. Kannan RY, Salacinski HJ, Ghanavi JE, et al. Silsesquioxane nanocomposites as tissue implants. *Plast Reconstr Surg*. 2007;119:1653–1662.
26. Kannan RY, Salacinski HJ, De Groot J, et al. The antithrombotic potential of a polyhedral oligomeric silsesquioxane (POSS) nanocomposite. *Biomacromolecules*. 2006;7:215–223.
27. Ghanbari H, de Mel A, Seifalian AM. Cardiovascular application of polyhedral oligomeric silsesquioxane nanomaterials: a glimpse into prospective horizons. *Int J Nanomedicine*. 2011;6:775–786.
28. Bao H, Wang E, Dong S. One-pot synthesis of CdTe nanocrystals and shape control of luminescent CdTe-cystine nanocomposites. *Small*. 2006;2:476–480.
29. Hong SY, Oh JE, Lee KH. Effect of d-amino acid substitution on the stability, the secondary structure, and the activity of membrane-active peptide. *Biochem Pharmacol*. 1999;58:1775–1780.
30. Law WC, Yong KT, Roy I, et al. Aqueous-phase synthesis of highly luminescent CdTe/ZnTe core/shell quantum dots optimized for targeted bioimaging. *Small*. 2009;5:1302–1310.
31. Rikans LE, Yamano T. Mechanisms of cadmium-mediated acute hepatotoxicity. *J Biochem Mol Toxicol*. 2000;14:110–117.
32. Wu J, Mather PT. POSS polymers: physical properties and biomaterials applications. *Polym Rev*. 2009;49:25–63.
33. Derfus AM, Chen AA, Min DH, Ruoslahti E, Bhatia SN. Targeted quantum dot conjugates for siRNA delivery. *Bioconjug Chem*. 2007;18:1391–1396.
34. Lovric J, Cho SJ, Winnik FM, Maysinger D. Unmodified cadmium telluride quantum dots induce reactive oxygen species formation leading to multiple organelle damage and cell death. *Chem Biol*. 2005;12:1227–1234.
35. Lovric J, Bazzi HS, Cuie Y, Fortin GR, Winnik FM, Maysinger D. Differences in subcellular distribution and toxicity of green and red emitting CdTe quantum dots. *J Mol Med*. 2005;83:377–385.
36. Su Y, He Y, Lu H, et al. The cytotoxicity of cadmium based, aqueous phase-synthesized, quantum dots and its modulation by surface coating. *Biomaterials*. 2009;30:19–25.
37. Su Y, Hu M, Fan C, et al. The cytotoxicity of CdTe quantum dots and the relative contributions from released cadmium ions and nanoparticle properties. *Biomaterials*. 2010;31:4829–4834.
38. Dubertret B, Skourides P, Norris DJ, Noireaux V, Brivanlou AH, Libchaber A. In vivo imaging of quantum dots encapsulated in phospholipid micelles. *Science*. 2002;298:1759–1762.
39. Derfus AM, Chan WC, Bhatia S. Intracellular delivery of quantum dots for live cell labeling and organelle tracking. *Adv Mater*. 2004;16:961–966.
40. Gao X, Cui Y, Levenson RM, Chung LW, Nie S. In vivo cancer targeting and imaging with semiconductor quantum dots. *Nat Biotechnol*. 2004;22:969–976.
41. Voura EB, Jaiswal JK, Mattoussi H, Simon SM. Tracking metastatic tumor cell extravasation with quantum dot nanocrystals and fluorescence emission-scanning microscopy. *Nat Med*. 2004;10:993–998.
42. Mattheakis LC, Dias JM, Choi YJ, et al. Optical coding of mammalian cells using semiconductor quantum dots. *Anal Biochem*. 2004;327:200–208.
43. Chan WC, Nie S. Quantum dot bioconjugates for ultrasensitive nonisotopic detection. *Science*. 1998;281:2016–2018.
44. McCusker C, Carroll JB, Rotello VM. Cationic polyhedral oligomeric silsesquioxane (POSS) units as carriers for drug delivery processes. *Chem Commun (Camb)*. 2005:996–998.
45. Cho SJ, Maysinger D, Jain M, Roder B, Hackbarth S, Winnik FM. Long-term exposure to CdTe quantum dots causes functional impairments in live cells. *Langmuir*. 2007;23:1974–1980.
46. Ma J, Chen JY, Zhang Y, et al. Photochemical instability of thiol-capped CdTe quantum dots in aqueous solution and living cells: process and mechanism. *J Phys Chem B*. 2007;111:12012–12016.
47. Zhang Y, Chen W, Zhang J, Liu J, Chen G, Pope C. In vitro and in vivo toxicity of CdTe nanoparticles. *J Nanosci Nanotechnol*. 2007;7:497–503.
48. Wang HQ, Zhang HL, Li XQ, Wang JH, Huang ZL, Zhao YD. Solubilization and bioconjugation of QDs and their application in cell imaging. *J Biomed Mater Res A*. 2008;86:833–841.
49. Xie R, Kolb U, Li J, Basche T, Mews A. Synthesis and characterization of highly luminescent CdSe-core CdS/Zn0.5Cd0.5S/ZnS multishell nanocrystals. *J Am Chem Soc*. 2005;127:7480–7488.
50. Zhang H, Sun P, Liu C, et al. L-Cysteine capped CdTeGÇöCdS coreGÇöshell quantum dots: preparation, characterization and immuno-labeling of HeLa cells. *Luminescence*. 2011;26:86–92.

## International Journal of Nanomedicine

### Publish your work in this journal

The International Journal of Nanomedicine is an international, peer-reviewed journal focusing on the application of nanotechnology in diagnostics, therapeutics, and drug delivery systems throughout the biomedical field. This journal is indexed on PubMed Central, MedLine, CAS, SciSearch®, Current Contents®/Clinical Medicine,

Submit your manuscript here: <http://www.dovepress.com/international-journal-of-nanomedicine-journal>

Dovepress

Journal Citation Reports/Science Edition, EMBase, Scopus and the Elsevier Bibliographic databases. The manuscript management system is completely online and includes a very quick and fair peer-review system, which is all easy to use. Visit <http://www.dovepress.com/testimonials.php> to read real quotes from published authors.